Signal Processing and Renewable Energy
December 2023, (pp. 59-67)
ISSN: 2588-7327
eISSN: 2588-7335

Ship Tracking Utilizing Propeller Noise with a Compact Hydro-phone Array

Mojgan Mirzaei Hotkani[1], Seyed Alireza Seyedin[1*]

[1] Department of Electrical Engineering, Ferdowsi University of Mashhad, Iran.

Received: 13-Aug-2023, Revised: 29-Sep-2023, Accepted: 18-Nov-2023.

Abstract
This study presents an innovative approach to ship tracking utilizing the analysis of propeller noise. It employs a hybrid technique that combines both time-domain and frequency-domain processing. In the frequency-domain aspect, the method utilizes matched field processing (MFP), which can be customized using diverse propagation models such as the normal modes, the image model, and the Lloyd-Mirror. Within this framework, an approximated time-domain frequency-limited covariance matrix is integrated, incorporating attributes of the Image propagation model, and coupled with the Multiple Signal Classification (MUSIC) algorithm. This integrated methodology leverages the strengths of both time-domain and frequency-domain strategies simultaneously. To validate the effectiveness of the proposed algorithm, actual data from a field trial conducted in collaboration with JASCO Applied Sciences Ltd at Duncan's Cove, Canada, in September 2020 is employed. The trial involved deploying a hydrophone array in the outbound shipping lane, which collected broadband noise data from various types of vessels, enabling the estimation of vessel bearings. The results from this real-world trial demonstrate the practical performance of the proposed algorithm.

Keywords: Matched Field Processing, MUSIC algorithm, Tracking ship noise, Underwater acoustic, Normal-mode model.

1. INTRODUCTION

Underwater ship-generated noise constitutes a substantial portion of the anthropogenic elements within marine ambient noise. This noise encompasses a broad spectrum of frequencies ranging from 20 Hz to 100 kHz, emanating from various sources including hydrodynamics, flow-induced noise, onboard machinery, and notably, propeller cavitation. [1].

The Characteristics of Propeller Noise

***Corresponding Authors Email:** seyedin@um.ac.ir

encompass a wide-ranging frequency spectrum, dominant frequencies correlated with propeller rotation speed, directional variations influenced by blade configuration, potential amplitude modulation, and hydrodynamic effects arising from the propeller's interaction with water.

Frequency Spectrum: Propeller noise demonstrates a wide-ranging frequency spectrum, encompassing frequencies from a few tens of Hertz to several kilohertz. The spectrum is characterized by the presence of multiple harmonics and broadband components.

Dominant Frequencies: The primary frequencies in propeller noise are contingent on the propeller's rotation speed and the number of blades. Typically falling within the low to mid-frequency range, these dominant frequencies play a crucial role in shaping the noise profile.

Directionality: Propeller noise exhibits directionality, signifying that noise levels fluctuate based on the observer's position in relation to the source. Factors like the configuration and arrangement of the propeller blades exert a notable influence on this directional characteristic.

Amplitude Modulation: Propeller noise may feature amplitude modulation, leading to variations in noise level over time. This modulation phenomenon can be attributed to alterations in ship speed, load, or other operational parameters.

Hydrodynamic Effects: The interaction between the propeller and the surrounding water, including the generation of vortices and cavitation, significantly contributes to the overall propeller noise. These hydrodynamic effects play a pivotal role in shaping the acoustic signature.

This paper focuses on ship-bearing tracking utilizing propeller-generated noise, employing an innovative passive localization algorithm based on Matched Field Processing (MFP). While a single sensor can effectively capture acoustic signatures by measuring pressure over time, localization requires a minimum of two hydrophones.

In specific array configurations, this setup allows for not only determining range but also azimuth and elevation bearings [2]. Several passive localization methods have been developed in recent years [3]. Existing passive localization methods can be categorized into four groups: 1) time delay of arrival (TDOA) [4], 2) direction of arrival (DOA) [5], 3) received signal strength, and 4) MFP [6]. MFP utilizes Green’s Function to generate a replica of the received signal, known for providing unparalleled accuracy, albeit accompanied by computational intricacies. The narrow-band Multiple Signal Classification (MUSIC) [7] algorithm, renowned for its high-resolution attributes, proves suitable for nearly all narrowband signals. While both the time-domain MUSIC and Multi-Channel Cross-Correlation Coefficient (MCCC) techniques are classified as high-resolution methods, their utility is constrained to free-space scenarios. Consequently, they lack applicability within the more intricate underwater models, namely Lloyd-Mirror, Image, and Normal-modes [8]. Several adapted iterations of MUSIC have been introduced to encompass broadband signals. These modifications encompass both time delay of arrival and attenuation considerations [9]. Indeed, when conducting localization through broadband signals, a comprehensive understanding of the propagating environment and its inherent characteristics becomes imperative.

Ocean acoustic propagation models commonly address the wave equation or Helmholtz equation, grounded in the underwater environment's boundary conditions within the frequency domain. These propagation solutions can be broadly classified into three categories, contingent on 1) the spectral composition of the source, 2) the depth of the region, and 3) the presence of range-dependent boundaries and objects in the deployment area. Lower frequencies allow for the neglect of absorption, thereby considerably simplifying the model's intricacy. In shallow water surroundings, the inclusion of multiple surface and seabed reflections becomes crucial, whereas deep water scenarios can often be approximated using a simplified Lloyd mirror pattern. Notably, in shallow water conditions, the sound speed profile can generally be assumed constant [8].

The structure of this paper is as follows: Section 2 describes a proposed time-frequency MUSIC algorithm for localizing the underwater active source; Section 3 reviews the experimental setup and data collection used to validate the results; in Section 4, the simulation results are analyzed; finally, Section 5 highlights the conclusions of this work.

2. PROPOSED TIME-FREQUENCY MUSIC ALGORITHM

MUSIC is a time-domain technique designed to estimate the time delay of arrival (TDOA) in unobstructed space through the employment of a hydrophone (or microphone) array comprising multiple elements. Let's consider $s(tk)$ is the time value of a given narrowband acoustic source at time tk, and is located at the point $p0 = (x0, y0, z0)$ in the Cartesian coordinate system. This value is received at the nth hydrophone at the location $p_n = (x_n, y_n, z_n)$ at time $tk + \tau n$, where τn is a delay. The transmit signal in the frequency domain is defined as [10]

$$S(\omega) = \frac{R_n(\omega)}{P(p_0, p_n, \omega)} \tag{1}$$

$R_n(\omega)$ is the Fast Fourier Transform (FFT) of the measured time signal $r_n(tk)$, and $P\ (p_0,\ p_n,\ \omega)$ is the channel frequency response that is obtained according to the underwater acoustic propagation model (for example using the image model or the Lloyd–mirror pattern) between the source position $p0$, and the sensor at position pn. At the baseband, the discrete frequency samples are equal to

$$\omega_l = l\Delta\omega, \qquad l = 0,1,\dots,\left\lfloor\frac{L}{2} - 1\right\rfloor,$$
$$\Delta t.\Delta\omega = \frac{2\pi}{L}, \tag{2}$$

where $\lfloor . \rfloor$ denotes the floor value of its argument, also, L is the length of the signal. In [10], a new localization algorithm was proposed based on the multi-channel cross-correlation coefficient (MCCC) localization algorithm where the frequency limited time-domain cross-correlation matrix (L×L) can be calculated using:

$$C_c(p) = \frac{1}{L}\sum_{k=0}^{L-1}(\bar{S}^T(t_k, p)\bar{S}(t_k, p)), \tag{3}$$

It was proven that:

$$\bar{S}^T(t_k,p)=\sum_{l=0}^{\frac{L}{2}-1}(\mathrm{Re}\{S_1(l,p)\}\mathrm{Re}\{S_2(l,p)\} -\mathrm{Im}\{S_1(l,p)\}\mathrm{Im}\{S_2(l,p)\}), \quad (4)$$

where Im$\{.\}$ denotes the imaginary part of its argument, and:

$$\begin{cases} S_1(l,p)=\dfrac{\Delta\omega(\varepsilon_l\bar{S}(\omega_l,p)e^{i\omega_t t_{min}})}{2\pi}, \\ S_2(l,p)=e^{i\frac{2\pi lk}{L}} \end{cases} \quad (5)$$

Also,

$$\bar{S}(\omega,p)=\left[\frac{R_1(\omega)|P(p,p_1,\omega)|}{P(p,p_1,\omega)}\cdots\frac{R_N(\omega)|P(p,p_N,\omega)|}{P(p,p_N,\omega)}\right]$$

is the FFT of s(tk, p), Note that | . | denotes the absolute value of its argument. The localization algorithm introduced in this study synergizes the frequency-time-constrained MCCC algorithm with the implementation of MUSIC localization, encompassing the following procedural steps.

1) Calculate the eigenvalues and the right eigenvectors of the time-domain cross-correlation matrix *C*c(p), where *C*c(p) is obtained from (3).

2) Sort the calculated eigenvalues based on the absolute values of their real parts in descending order, and then sort the corresponding eigenvectors in order of the sorted eigenvalues. The eigenvalues are denoted ***V*** s(*p*).

3) Eliminate the first eigenvector and obtain the matrix of remaining eigenvectors represented as:

$$\bar{V_s}(p)=[V_{s2}(p)V_{s3}(p)\cdots V_{sN}(p)], \quad (6)$$

4) Estimate the location of source *p*0 = (*x*0, *y*0, *z*0) using:

$$\hat{p}_0=\arg\max_p\{(\textstyle\sum_{n=2}^{N}(V_{s\,n}^T(p).C_c(p).V_{s\,n}(p)))^{-1}\} \quad (7)$$

3. EXPERIMENTAL SETUP AND DATA COLLECTION

The data under examination in this manuscript originated from a sensor deployed in a high-traffic shipping lane for a span of 21 days. This experiment was a collaborative effort with JASCO Applied Sciences, conducted in Duncan’s Cove, Nova Scotia, Canada, in September 2020. The precise coordinates for the hydrophone array’s location are 44.4803◦N, 63.513115◦W, at a depth of 70 meters. Positioned on the ocean floor, at approximately 900 meters from the traffic lanes along the Nova Scotian coast, the hydrophone array consisted of four elements, a set of AMAR G4 SeaLander devices. This arrangement facilitated the systematic collection of broadband noise data from diverse ship classifications, essential for precise ship tracking. Operating at a uniform sampling frequency of 128 kHz, all elements were meticulously synchronized using a typical clock. The configuration comprised three hydrophones organized in a planar array formation, with an additional hydrophone strategically positioned above to establish a two-element vertical array in conjunction with one of the existing elements. Fig. 1 shows the schematic of the hydrophone array. Their position using a Cartesian coordinate is shown in Table. I. Note that the sea depth in the area was 71.628 m.

Table 1. ***Coordinates of Hydrophones in Meter.***

	x_n	y_n	z_n
H1	-0.06	0.545	70.3
H2	-0.07	0.045	70.3
H3	0	0	70
H4	0.450	0.03	70.315

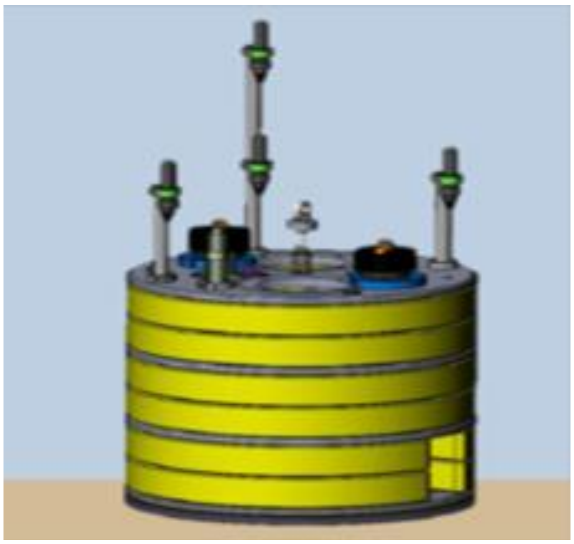

Fig. 1. Drawing of the hydrophone array.

The experiment spanned 21 days, commencing on September 8 and concluding on September 29, 2020. Throughout this duration, numerous vessels traversed the area, with their acoustic emissions being captured by the hydrophone array. To rigorously evaluate the precision of the proposed methodology, the precise location of each passing ship was continuously acquired across the experimental expanse. Notably, shipping data was sourced within a defined square region of 10×10 km^2 near the sensor location through MarineTraffic[1] (Automated Identification System data), enabling a comprehensive assessment of the algorithm's accuracy.

Fig. 2 indicates the spectrogram and sound pressure level of the recorded acoustic noise for the complete duration of the trial. In the upper portion of the figure, the SPL is analyzed for four different decades between 10^1 and 10^4. As can be observed, the data on September 23 shows a large increase in energy due to Hurricane Teddy. Propeller noise from nearby ships can be heard on other days.

This paper employs shipping noise data from September 10 to verify the accuracy of the localization algorithm. The designated frequency band for the shipping noise ranges between 400 and 2500 Hz.

4. PERFORMANCE ANALYSIS

Within this section, the performance evaluation of the localization algorithm is undertaken using real-world data. Leveraging the distinctive geometry of the array, remarkable precision in determining ship bearings is demonstrated by the algorithm. Nevertheless, achieving accurate range estimations requires a greater number of vertical elements.

Illustrating this aspect, an exemplary case is provided by the CMA CGM Brazil, one of the world's largest cargo vessels, which anchored at Halifax harbor on September 10, 2020. With an immense capacity of 15,000 containers, the ship features dimensions of 366 meters in length and 51 meters in width. By traversing the predefined AIS data region, a combination of received AIS data and acoustic sensor data enabled comprehensive tracking of this immense vessel. Fig. 3 displays a one-second time signal and its corresponding spectrum for the propeller noise emitted by the CMA CGM Brazil ship. Fig. 4 illustrates a segment of the ship's tracked route, denoted by geographical coordinates sourced from AIS data. In order to compare the proposed methods with the conventional frequency-domain MUSIC in terms of resolution, a complete sweep of bearing (-179 to 180 deg) in the far field is conducted during the third minute of the recorded window. Fig. 5 presents the normalized received energy at the hydrophone array as a function of bearing for both the conventional MUSIC and the proposed method.

Using the proposed method with the Image model, the angular position of this ship is tracked for about 8 minutes. Fig. 6 shows the corresponding results of the conventional frequency-domain MUSIC and the proposed method compared with the angular position that was obtained from the AIS data. As can be seen from Fig. 6 and Fig. 5, the proposed method provides more accurate results than conventional frequency-domain MUSIC.

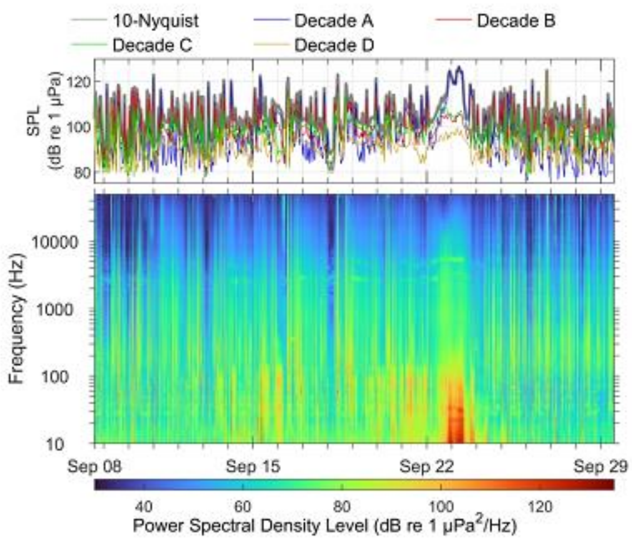

Fig. 2. Spectrogram and Sound Pressure Level (SPL) at the output of the first sensor.

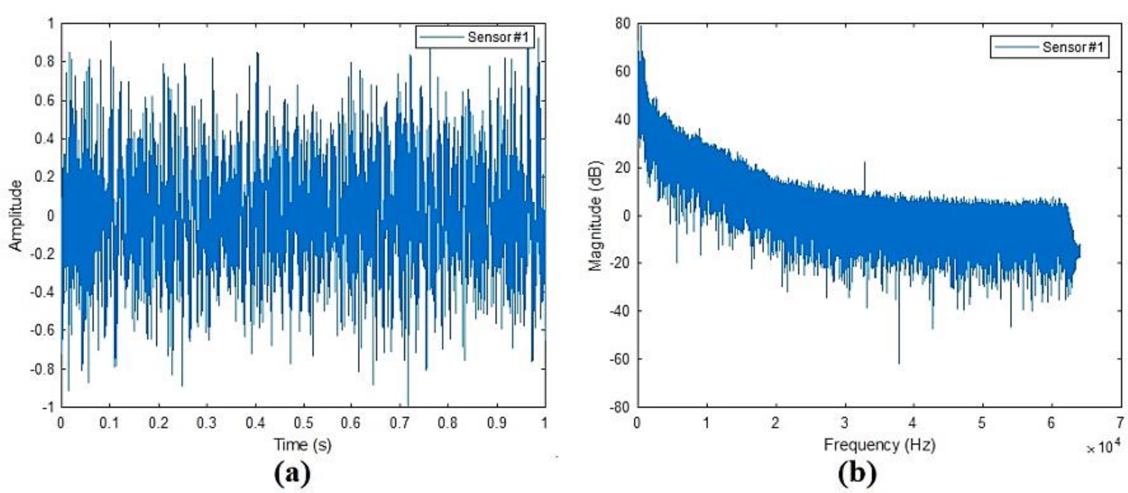

Fig. 3. A one-second time signal and its spectrum of the propeller noise of the CMA CGM Brazil ship. a time-domain signal b Frequency-domain signal.

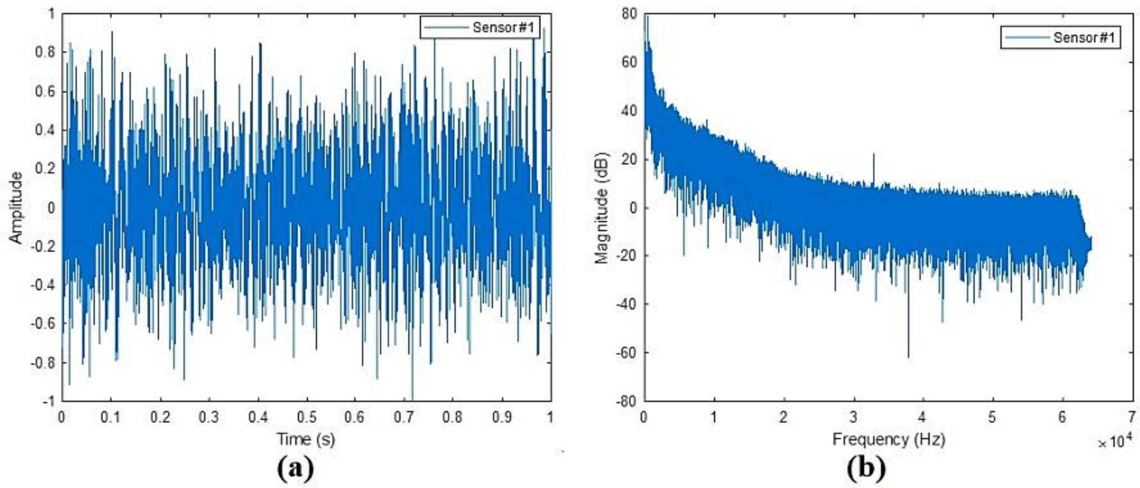

Fig. 3. A one-second time signal and its spectrum of the propeller noise of the CMA CGM Brazil ship. a time-domain signal b Frequency-domain signal.

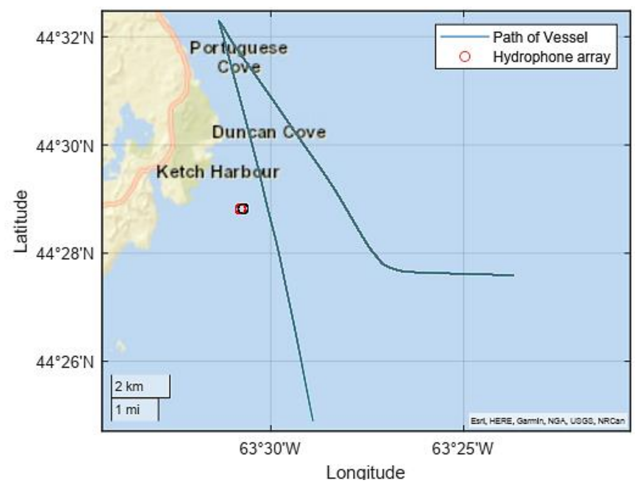

Fig. 4. The partial of the tracked route of the Brazil ship at the geographical coordinates.

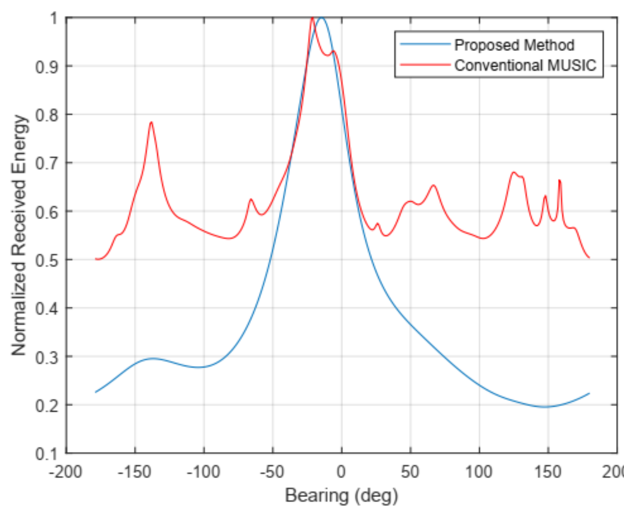

Fig. 5. Normalized received energy as a function of bearing.

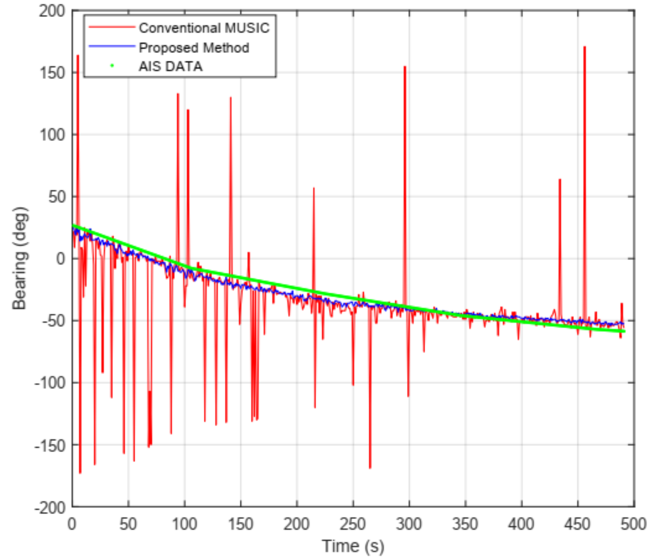

Fig. 6. Tracking results for the CMA CGM Brazil ship.

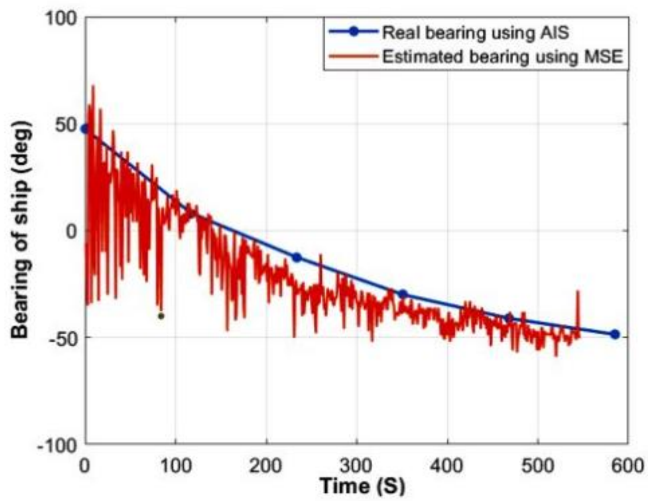

Fig. 7. Estimating the bearing of the CMA CGM Brazil using the Mean Squared Error algorithm.

The conventional MFP localization algorithm is simulated to compare with the proposed localization algorithm as shown in Fig. 7. The conventional MFP uses the mean squared error (MSE) to estimate the location of the source, expressed $p\hat{}0 = (x0, y0, z0)$ as:

$$\widehat{p_0} = \arg\max_p \left\{ \left(\sum_i \sum_{\vartheta=1}^{N} \sum_{n=\vartheta+1}^{N} |\Gamma_{\vartheta\, n}(p, \omega_i)|^2 \right)^{-0.5} \right\} \quad (8)$$

where

$$\Gamma_{\vartheta\, n}(p, \omega_i) = \frac{P(p, p_\vartheta, \omega_i) P(p, p_\vartheta, \omega_i)^H}{|P(p, p_\vartheta, \omega_i) P(p, p_\vartheta, \omega_i)^H|} - \frac{R_\vartheta(\omega_i) R_n(\omega_i)^H}{|R_\vartheta(\omega_i) R_n(\omega_i)^H|}. \quad (9)$$

where $P\ (p,\ p1,\ \omega_i)$ and $R_n(\omega_i)$ represent the chosen propagation model and the measured signal at the nth hydrophone, respectively. The estimated bearing in Fig. 7 is very noisy and has not been able to track AIS data well.

5. CONCLUSION

In conclusion, this paper presents an innovative approach by integrating an approximated frequency-limited cross-correlation matrix into the time-domain MUSIC framework for localizing underwater acoustic sources. The results highlight the method's adept combination of the advantageous characteristics inherent in both time-domain and frequency-domain localization techniques. Its success lies in its ability to distinguish distinct sources across varying frequencies while focusing on specific frequency ranges or precise values. The algorithm achieves exceptional resolution by accounting for environmental complexities, all within a computationally feasible timeframe. The validation of this algorithm's effectiveness is confirmed through its application to real-world ship noise data. By capturing propeller noise, the algorithm adeptly pinpoints ships, affirming its practical utility and robustness. In essence, this approach harmonizes precision, computational efficiency, and adaptability, paving the way for enhanced underwater acoustic source localization.

REFERENCES

[1] J. Sung Park, D. Kang, S. Cho, Noise directionality estimated using ship tracking data in the Southern Sea of Korea, The Japan Society of Applied Physics, 2018.

[2] Luo J, Han Y, Fan L. Underwater Acoustic Target Tracking: A Review Sensors (Basel). 2018;18(1):112. Published 2018 Jan 2.

[3] J. Li, Q. H. Lin, K. Wang, and C. Y. Kang, Performance Analysis for Focused Beamformers in Passive Underwater Acoustic Localization, IEEE Access, 2018.

[4] J. Benesty, J. Chen, Y. Huang, Microphone Array Signal Processing, Springer Berlin Heidelberg, 2008.

[5] Van Trees, H.: Optimum Array Processing Part IV. Wiley-Interscience, 2002.

[6] P. N. Tran and K. D. Trinh, Adaptive Matched Field Processing for Source Localization Using Improved Diagonal Loading Algorithm, Acoust. Aust., 2017.

[7] J. P. Dmochowski, J. Benesty and S. Affes: ‘Broadband MUSIC: opportunities and challenges for multiple source localization’, *In Proc. IEEE WASPAA*, 2007, pp. 18-21.

[8] F. B. Jensen, W. A. Kuperman, M. B. Porter and H. Schmidt: ‘Computational Ocean acoustics’ (Springer Science & Business Media, 2011.

[9] P. Vallet, X. Mestre and P. Loubaton, *Performance Analysis of an Improved MUSIC DoA Estimator*, in IEEE Transactions on Signal Processing, vol. 63, no. 23, pp. 6407-6422, Dec.1, 2015, doi: 10.1109/TSP.2015.2465302.

[10] M. Mirzaei Hotkani, J.-F. Bousquet, S.A. Seyedin, B. Martin, E. Malekshahi, *Underwater Target Localization Using Opportunistic Ship Noise Recorded on a Compact Hydrophone Array*, Acoustics 2021,